

## Supporting Information

### Dually Reactive Multilayer Coatings Enable Orthogonal Manipulation of Underwater Superoleophobicity and Oil Adhesion via Post-Functionalization

Angana Borbora<sup>a</sup>, Robert L. Dupont<sup>b</sup>, Yang Xu<sup>b</sup>, Xiaoguang Wang<sup>b,c\*</sup>, Uttam Manna<sup>a,d,e\*</sup>

#### Experimental Section:

**Materials:** Branched polyethyleneimine (BPEI; molecular weight is 25,000 Da), tripentaerythritol pentaacrylate (5AcI; molecular weight is 524.21 g mol<sup>-1</sup>), 3-(dimethylamino)-1-propylamine (DMAPA), 2-carboxyethyl acrylate (CEA), butyl acrylate, hexyl acrylate, octyl acrylate, decyl acrylate, lauryl acrylate, octadecyl acrylate 2-(dimethylamino)ethyl acrylate, 2-hydroxyethyl acrylate, hexylamine, and hexyl acrylate, Sodium dodecyl sulfate (SDS), sodium tetradecyl sulfate (STS), decyltrimethylammonium bromide (C<sub>10</sub>TAB), dodecyltrimethylammonium bromide (DTAB), hexadecyltrimethylammonium bromide (HTAB), cholic acid, and L-ascorbic acid (AA) were purchased from Sigma Aldrich, Bangalore, India. D-glucamine, β-alanine, sodium decyl sulfate (SDeS), uric acid (UA), and octyl acrylate were acquired from TCI chemicals (India) Pvt. Ltd. Ethanol was purchased from TEDIA Company (USA). Tetrahydrofuran (THF) was obtained from RANKEM, Maharashtra, India. Dichloroethane (DCE) was acquired from Loba Chemie Pvt. Ltd., India. Di-sodium hydrogen phosphate dihydrate (Na<sub>2</sub>HPO<sub>4</sub>·2H<sub>2</sub>O) and sodium phosphate monobasic monohydrate (NaH<sub>2</sub>PO<sub>4</sub>·H<sub>2</sub>O), Dimethyl sulfoxide (DMSO) were obtained from Merck Life Science Pvt. Ltd, Mumbai. PBS buffer was prepared by mixing Na<sub>2</sub>HPO<sub>4</sub>·2H<sub>2</sub>O and NaH<sub>2</sub>PO<sub>4</sub>·H<sub>2</sub>O following the standard sodium phosphate buffer preparation protocol.

#### Characterization:

The underwater oil contact angles were measured at five different positions for each sample using a KRUSS Drop Shape Analyzer-DSA25 instrument at ambient temperature. The surface topography of the fabricated multilayer was visualized using a field emission electron microscope (FESEM, Sigma Carl Zeiss). All samples were first subjected to gold sputtering to form a thin gold layer prior to imaging. Attenuated total reflection Fourier transform infrared (ATR-FTIR) spectra were recorded using PerkinElmer UATR Two at ambient conditions. Digital photographs were captured using a Canon powershot SX540HS digital camera. The adhesive forces of the oil droplets on the multilayer coatings were measured using a highly sensitive microelectromechanical balance system (Kruss force tensiometer, Germany). Atomic force microscope (AFM) images were acquired using an OXFORD Cypher Atomic Force Microscope. Fluorescence micrographs were obtained using a ZEISS Axio Vert.A1 inverted microscope. Milli-Q water was used for all experiments.

### **Preparation of Dual-Reactive Multilayer Coatings:**

Two ethanol solutions of 5Acl ( $132.5 \text{ mg mL}^{-1}$ ) and BPEI ( $50 \text{ mg mL}^{-1}$ ) were prepared and then mixed to obtain a solution with a 1:10 ratio of BPEI:5Acl. After 15 minutes, the mixture was used to initiate the formation of the chemically reactive nanocomplex (CRNC). The multilayer coatings were prepared through a layer-by-layer (LbL) deposition process. First, a glass substrate ( $7.5 \text{ cm} \times 1.0 \text{ cm}$ ) was placed in the BPEI solution for 10 seconds. Next, the substrate was removed and washed with an ethanol bath for 10 seconds, followed by a second ethanol bath for another 10 seconds to remove the unabsorbed or loosely absorbed polymers. Subsequently, the substrate was dipped in a dispersion of growing CRNC solution in ethanol for 10 seconds and then washed using two ethanol baths. This cycle was repeated 20 times to fabricate a porous polymeric coating of 20 BPEI/CRNC bilayers. Each BPEI/CRNC layer is referred to as a 'bilayer' in the main text. To form a smooth multilayer coating, we used a similar LbL deposition to prepare 5 bilayers of BPEI/5Acl.

### **Post-Modification of Multilayer Coatings Using Amine and Acrylate:**

The multilayers of BPEI/CRNC contain residual acrylate and primary amine groups, which provide an opportunity for post-modification with other chemical functionalities via a 1,4-conjugate addition reaction at ambient conditions. The residual acrylates of the multilayers were post-modified with hydrophilic amines including 3-(dimethylamino)-1-propylamine (DMAPA,  $25 \text{ }\mu\text{L/mL}$  in ethanol),  $\beta$ -alanine ( $5 \text{ mg/mL}$  in water), and glucamine ( $2.5 \text{ mg/mL}$  in DMSO) by exposing the multilayer coatings in the respective solutions overnight at ambient conditions. After washing the multilayers with ethanol and drying with air, the mono-functionalized multilayers exhibited an underwater non-adhesive superoleophobicity. For further modification of the residual amine groups of the mono-functionalized multilayers, the multilayer coating was exposed to an ethanol solution consisting of a hydrophilic acrylate, 2-carboxyethyl acrylate ( $25 \text{ }\mu\text{L/mL}$ ), or hydrophobic alkyl acrylates (butyl acrylate ( $25 \text{ }\mu\text{L/mL}$ ), hexyl acrylate ( $25 \text{ }\mu\text{L/mL}$ ), octyl acrylate ( $25 \text{ }\mu\text{L/mL}$ ), decyl acrylate ( $25 \text{ }\mu\text{L/mL}$ ), lauryl acrylate ( $25 \text{ }\mu\text{L/mL}$ ) or octadecyl acrylate ( $25 \text{ }\mu\text{L/mL}$ )) overnight at ambient conditions. After washing with ethanol and drying with air, the obtained dual-functionalized superoleophobic coatings exhibited either oil adhesion ( $\text{CAH} > 10^\circ$ ) or non-adhesion ( $\text{CAH} < 10^\circ$ ), depending on the hydrophobicity of the acrylates.

### **Fabrication of Patterned Underwater Superoleophobic Surfaces:**

To distinguish between the charge types of the head groups of surfactants, multilayer coatings with patterned superoleophobicity were fabricated through strategic modification of the residual amines and acrylates of the multilayer coating on the glass substrate ( $7.5 \text{ cm} \times 2.5 \text{ cm}$ ). Specifically, after preparation of the BPEI/CRNC multilayers using the above described LbL process, half of the multilayer was treated with an ethanol solution of DMAPA ( $25 \text{ }\mu\text{L/mL}$ ) using a paintbrush, followed by rinsing with ethanol. Next, the other half of the multilayer coating was modified with  $\beta$ -alanine ( $5 \text{ mg/mL}$  in water) and 2-carboxyethyl acrylate ( $25 \text{ }\mu\text{L/mL}$  in ethanol), followed by drying with air.

### **Non-covalent, Reversible Modifications of Multilayer Coatings with Ionic Surfactants and Bile Acid:**

The patterned superoleophobic interfaces modified with DMAPA (MI-1) and with  $\beta$ -alanine and CEA (MI-2) were immersed in aqueous solutions of ionic surfactants (either cationic or anionic). The oil adhesion behaviors were measured by monitoring the change in the CAH of an underwater  $5 \text{ }\mu\text{L}$  beaded oil (DCE) droplet. The concentration of the ionic surfactants was varied between  $0 \text{ }\mu\text{M}$  and

600  $\mu\text{M}$ , and the pH of the prepared solutions was adjusted using either HCl or NaOH. To detect cholic acid, the glucamine/alkyl acrylate-modified multilayer coatings were immersed in the cholic acid solution prepared in sodium phosphate buffer solution with a pH of 7. The change in the roll-off angle and the CAH of a 5  $\mu\text{L}$  beaded oil (DCE) droplet on the coatings was measured as a function of cholic acid concentration.

## **Chemical, thermal, and physical stability of the underwater superoleophobic Properties**

### *Chemical and thermal stability:*

The multilayer coatings, which were post functionalized with appropriate hydrophilic molecules, were immersed in different harsh and chemically complex conditions, like alkaline solutions (0.1M  $\text{NH}_3$ ; pH 11), acidic solutions (0.1M HCl; pH 1), SDS solutions (1mM), DTAB solutions (1mM), 5% BSA solutions, and artificial sea-water for a prolonged 10 days. The artificial sea-water was prepared by mixing  $\text{MgCl}_2$  (0.226g),  $\text{MgSO}_4$  (0.325g), NaCl (2.673g) and  $\text{CaCl}_2$  (0.112g) in 100ml of deionized water. The underwater oil wettability in the respective materials was examined visually and the contact angle was measured after exposure to one of the mentioned chemically harsh media for 10 days.

To investigate the thermal stability of the modified coatings, the coatings were subjected to  $-5^\circ\text{C}$  and  $90^\circ\text{C}$  for 10 days and the underwater oil wettability was examined with contact angle measurements.

### Physical durability:

#### *1. Sand drop test:*

The modified interfaces were placed on a  $\sim 45^\circ$  tilted surface using an adhesive tape in air, and a continuous stream of sand grains (50 g) was poured from a height of 20 cm using a funnel. Anti-wetting properties of the material were examined by taking contact angle measurements and digital images before and after performing the sand drop test.

#### *2. Adhesive Tape Peeling Test:*

One adhesive surface of a double-sided adhesive tape was adhered to a glass microscope slide before the other was brought in contact with the modified multilayer coating. A 100g load was placed on the system to further facilitate a uniform contact of the polymeric coating against the adhesive surface. After 15 minutes, the polymeric multilayer coated glass slides were manually peeled off from the adhesive surface, and the anti-wetting properties in the coatings were investigated in detail.

#### *3. Finger Rubbing Test:*

The modified interfaces were rubbed with a finger back and forth for 20 times, and the underwater oil wettability was investigated in detail.

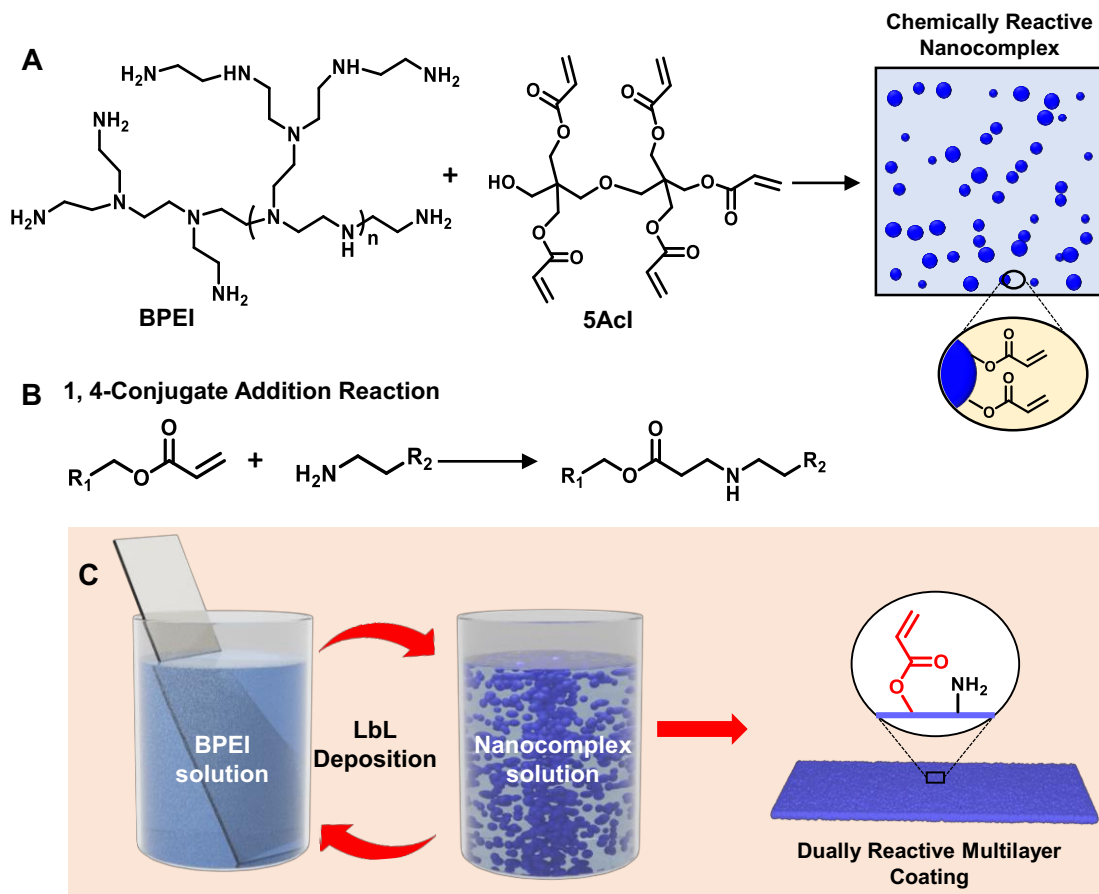


**Figure S1.** (A) Schematic representing the formation of the chemically reactive nano-complexes after mixing of BPEI and 5AcI in ethanol, where available amine and acrylate spontaneously reacted through 1, 4-conjugate addition reaction (B). (C) The covalent layer-by-layer (LbL) deposition of BPEI and nanocomplexes on the glass substrate yielded the dually reactive multilayer coating.

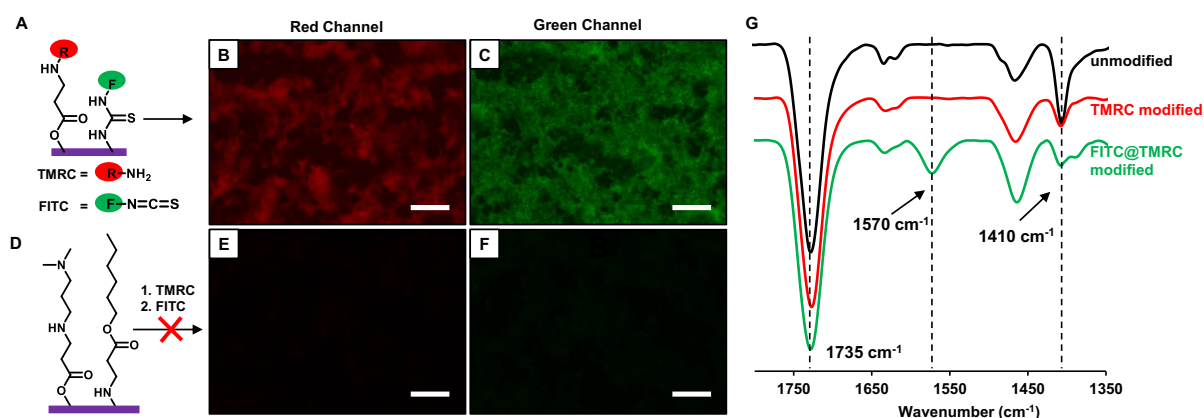


**Figure S2.** (A–C) Schematic illustration (A) and corresponding fluorescence micrographs (B, C) of the duallyreactive multilayer coatings after sequential treatments with TMRC and FITC. (D–F) Schematic illustration (D) and corresponding fluorescence micrographs (E, F) of DMAPA/hexyl acrylate–modified multilayer coatings after sequential modification using TMRC and FITC. The excitation and emission wavelength of TMRC and FITC are 544 – 571 nm and 495 – 519 nm, respectively. Scale bars, 50  $\mu\text{m}$ . (G) ATR–IR spectra before (black) and after TMRC modification (red) and TMRC/FITC modification (green) of the multilayer coating. The depletion of the IR signature at  $1,410\text{ cm}^{-1}$  is noted with reference to the carbonyl stretching at  $1,735\text{ cm}^{-1}$ , which is caused by the covalent modification of the residual acrylate groups with the primary amine of TMRC. The appearance of an IR peak at  $1,570\text{ cm}^{-1}$  (green) is due to the mutual chemical reaction between the isothiocyanate group of FITC and the residual amine.

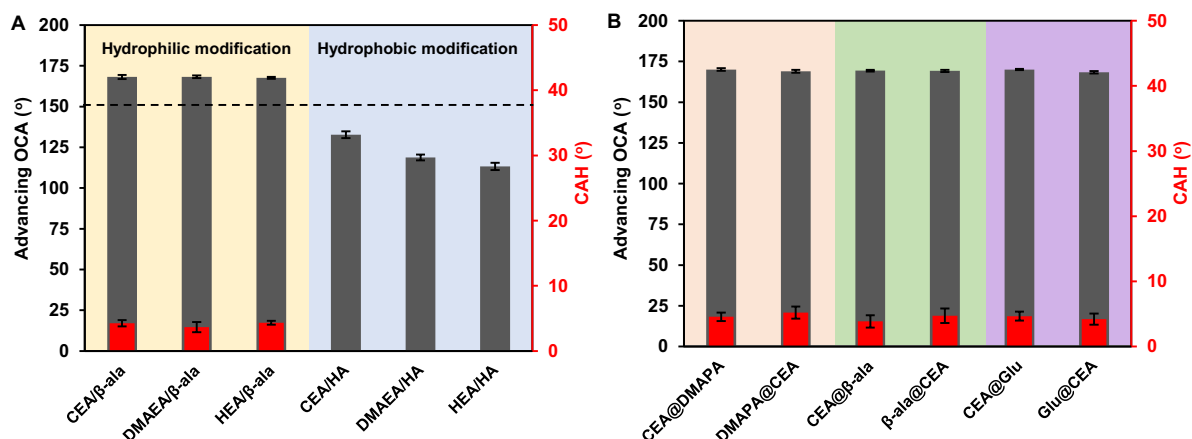


**Figure S3.** (A) Advancing oil contact angle (OCA ; gray bars) and CAH (contact angle hysteresis; red bars) of an oil droplet on 2-carboxyethylacrylate (CEA), 2-(dimethylamino)ethyl acrylate (DMAEA), and 2-hydroxyethylacrylate (HEA)-modified multilayer coatings after further modification with either hydrophilic β-alanine (β-ala) or hydrophobic hexylamine (HA). (B) Advancing OCA (gray bars) and CAH (red bars) of an oil droplet on the hydrophilic amine (DMAPA, β-ala, or Glu) and hydrophilic acrylate (CEA) modified multilayer coating. We note here that the changes in the sequence of the chemical modifications have no measurable impact on the final underwater oil wettability. The volume of the beaded oil droplets was 5 μL. Error bars represent standard deviations with n = 3 for each data point.

**Table S1:** surface energy values of the unmodified & modified interfaces

Multilayer coatings	surface energy
unmodified	40 ± 1.56 mN/m
DMAPA modified	70.29 ± 0.87 mN/m
β-alanine/CEA modified	71.81 ± 0.96 mN/m
Glucamine/Lauryl acrylate modified	65.87 ± 2.06 mN/m

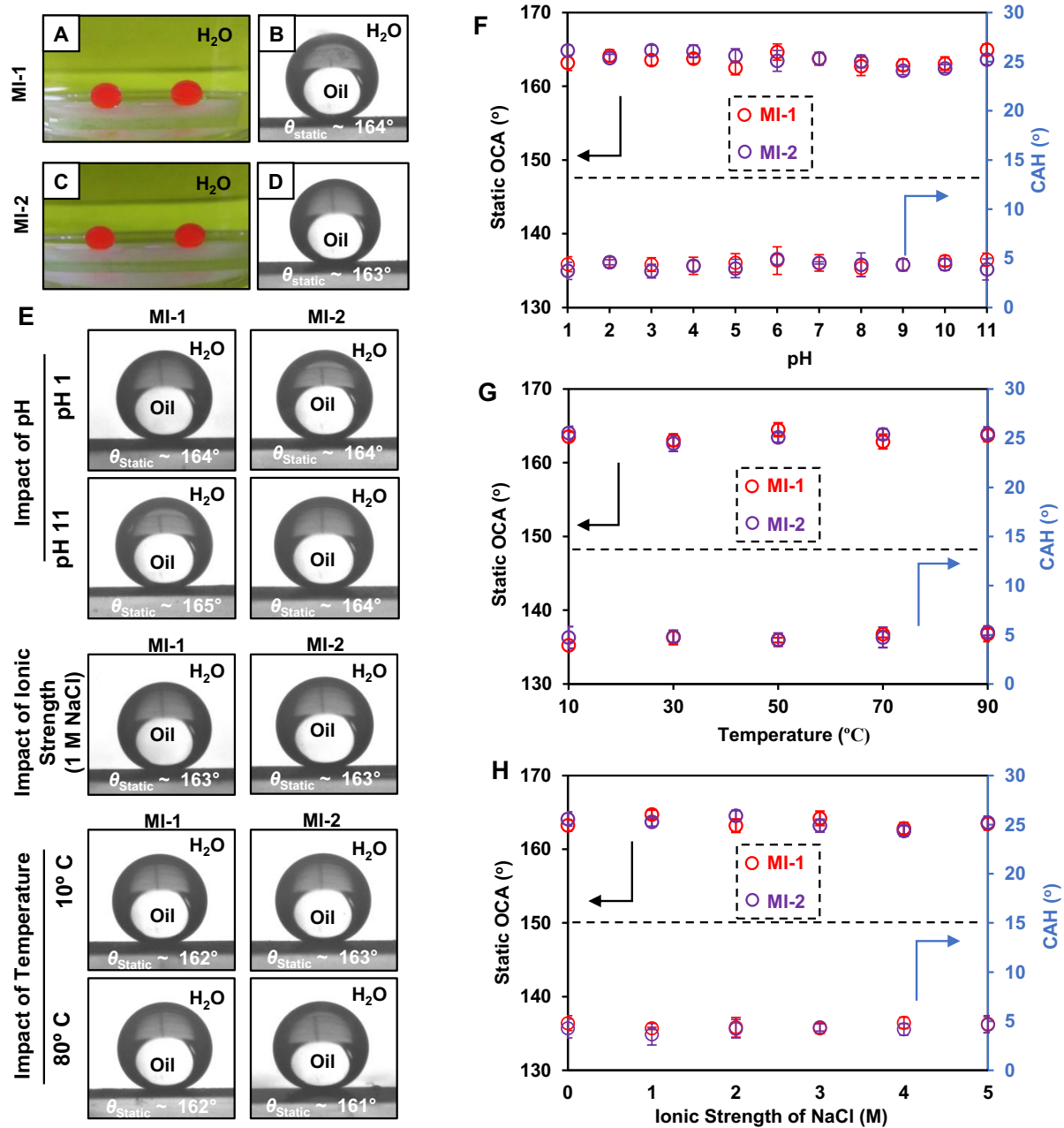


**Figure S4.** (A–D) Digital images (A, C) and contact angle goniometer images (B, D) of the beaded oil droplets on the DMPA-modified (MI-1; A–B) and  $\beta$ -alanine/CEA-modified (MI-2; C–D) multilayer coatings. (E) Contact angle goniometer images showing the static underwater OCA of beaded droplets MI-1 and MI-2 under various severe conditions—including extremes of pH (1 & 11) ionic strength (1M; NaCl) and extremes of temperatures. (F–H) Static OCA and CAH of beaded oil droplets on MI-1 and MI-2 modified surfaces as a function of pH (F), NaCl concentration (G), and temperature (H). Error bars represent standard deviations with  $n = 3$  for each data point. The volume of the beaded oil droplets was 5  $\mu$ L.

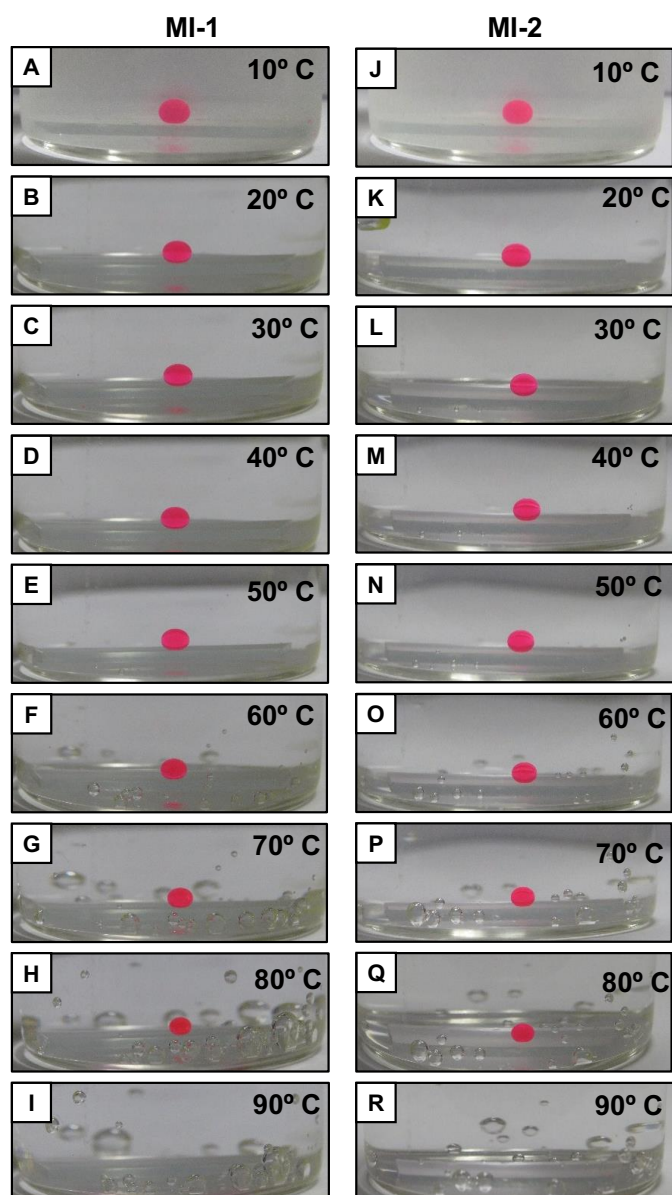


**Figure S5.** Photographs of oil droplets on the MI-1 (A–I) and MI-2 (J–R) superoleophobic coatings underwater at different temperatures. The oil droplets remained spherical due to the extreme oil repellency of the underwater superoleophobic multilayers before the complete evaporation of the oil- droplet at high temperatures. The volume of the beaded oil droplets was 15  $\mu\text{L}$ .

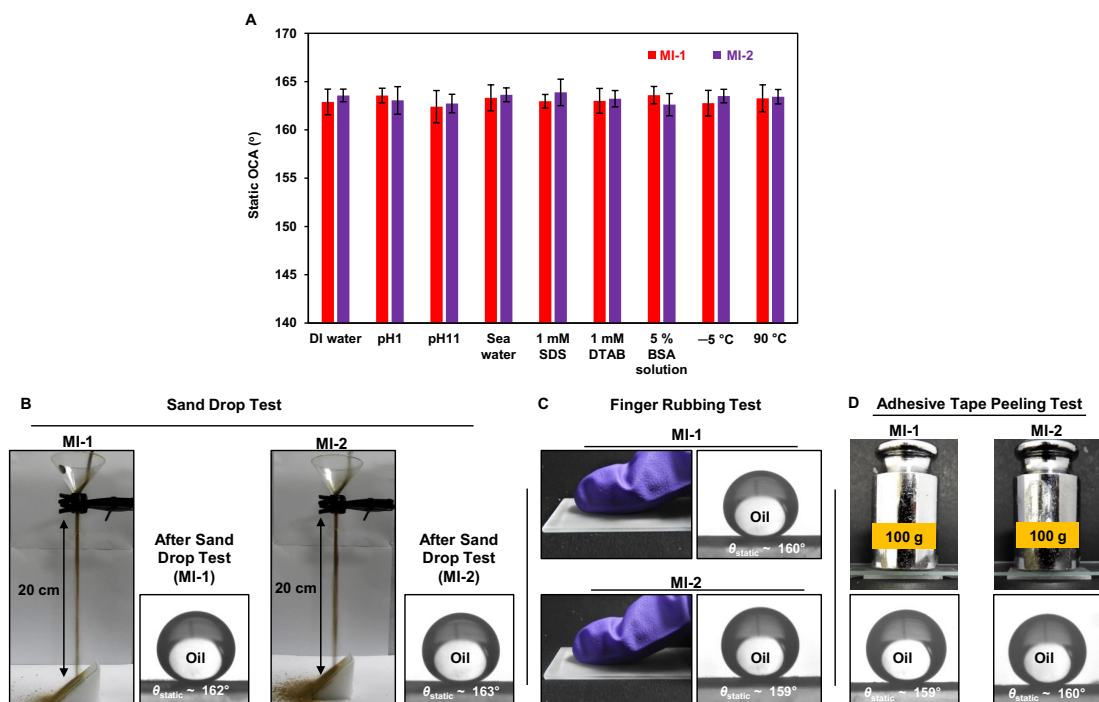


**Figure S6.** (A) The graph represents the static oil contact angles on the MI-1 and MI-2 after exposing the coatings to various chemically contaminated aqueous phases and temperatures ( $-5^{\circ}\text{C}$  &  $90^{\circ}\text{C}$ ). The measurement was taken after 10 days of continuous exposure of the coating to the respective conditions. Error bars represent standard deviations with  $n = 3$  for each data point. (B) Digital images of the sand drop test and contact angle goniometer images of the beaded oil droplets underwater on MI-1 and MI-2 after carrying out the sand drop test. (C) Digital images of the finger rubbing test and contact angle goniometer images of the beaded oil droplets underwater on MI-1 and MI-2 after the test. (D) Digital images and contact angle goniometer images of beaded oil droplets on the MI-1 and MI-2 after performing the adhesive tape test.

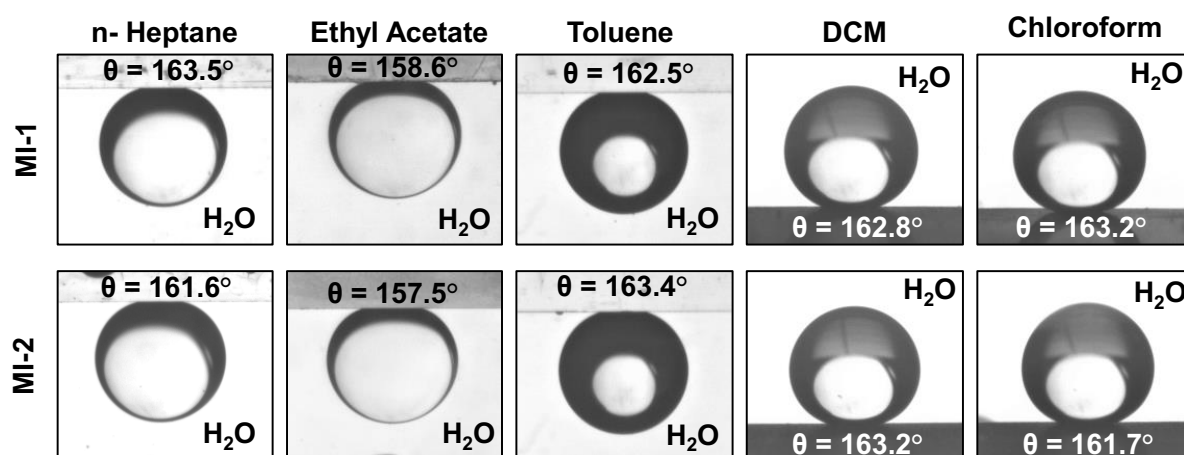


**Figure S7.** Beaded droplets of various water-immiscible organic phases remained extremely repellent on both the MI-1 and MI-2 surfaces.

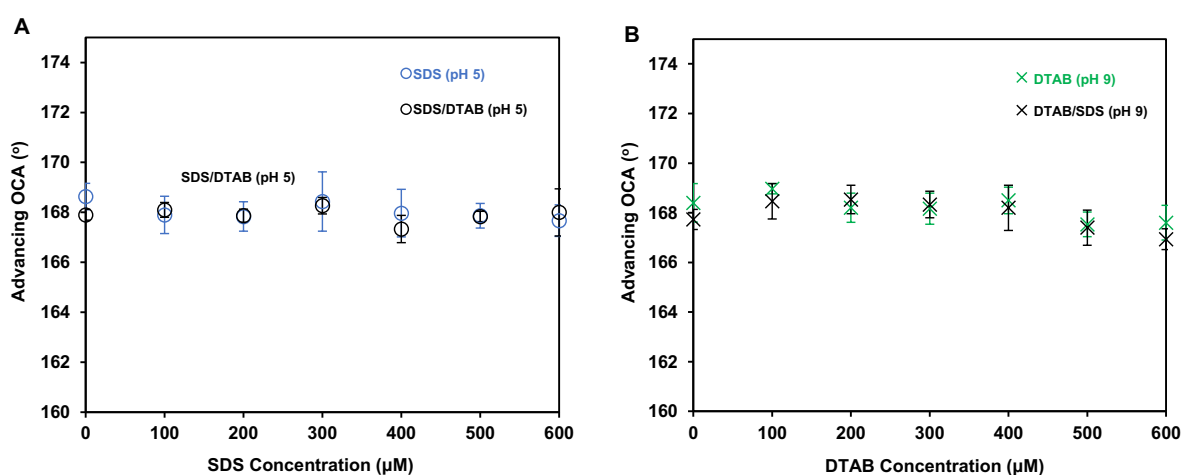


**Figure S8.** (A) Advancing-OCA of the beaded droplets on underwater MI-1 superoleophobic coatings as a function of SDS concentration at a pH of 5 in the presence of a fixed amount DTAB (concentration of 200 μM). (B) Advancing-OCA of beaded droplets on underwater MI-2 superoleophobic coatings as a function of DTAB concentration at a pH of 9 in the presence of a fixed amount of SDS (concentration of 200 μM). Error bars represent standard deviations with  $n = 3$  for each data point.

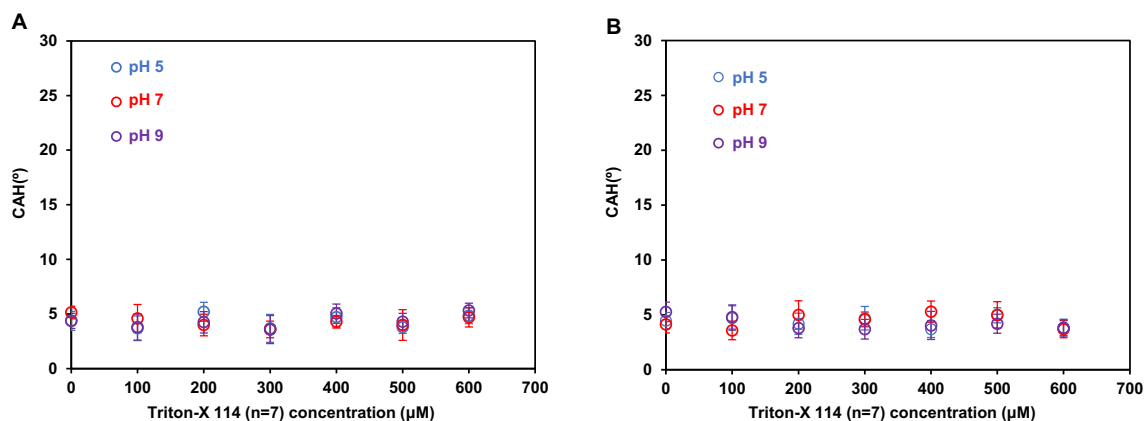


**Figure S9.** (A-B) Underwater CAH of the beaded droplets of oil on MI-1 (A) and MI-2 (B) as a function of Triton-X 114 concentration at pH of 5, 7, and 9. Error bars represent standard deviations with  $n = 3$  for each data point. The volume of the beaded oil droplets was  $5 \mu\text{L}$ .

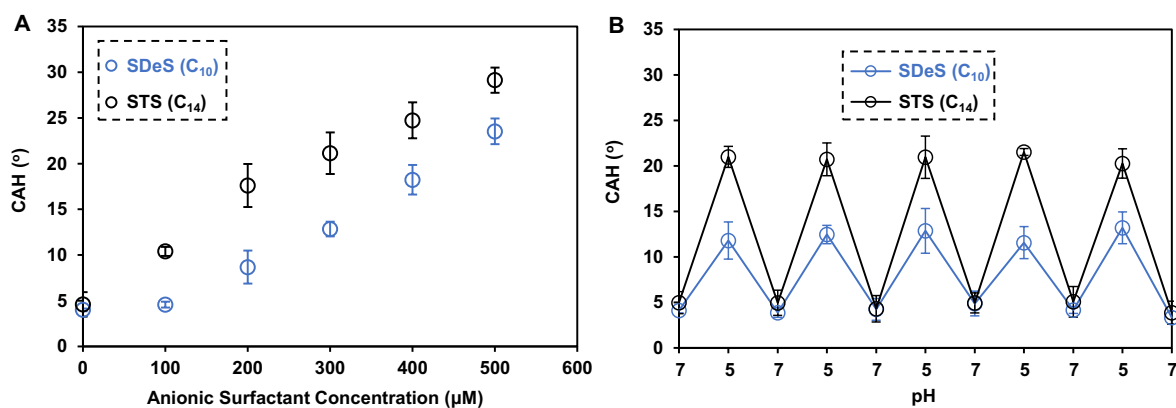


**Figure S10.** (A) The CAH of oil droplets on underwater MI-1 superoleophobic coatings as a function of the concentration of anionic surfactants with varying hydrocarbon tail length (sodium decyl sulfate (SDeS) and sodium tetradecyl sulfate, (STS)) at a pH of 5. (B) The reversible manipulation of the CAH of underwater superoleophobic coatings (MI-1) in anionic surfactant aqueous solutions obtained by switching the pH between 5 and 7. The concentration of SDeS and STS was  $300 \mu\text{M}$ . Error bars represent standard deviations with  $n = 3$  for each data point. The volume of the beaded oil droplets was  $5 \mu\text{L}$ .

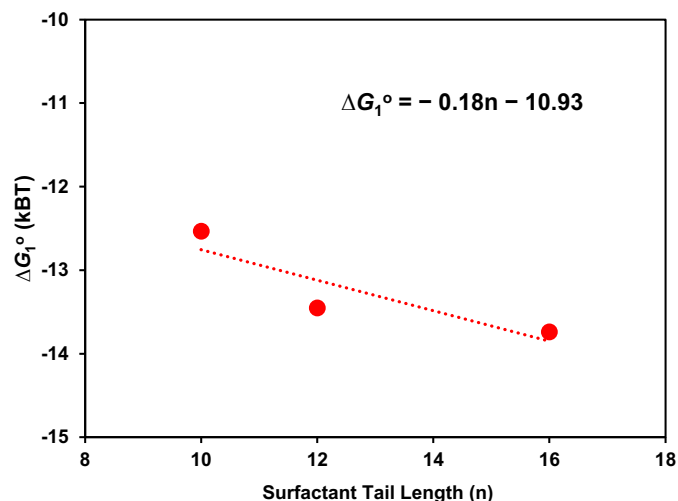


**Figure S11.** Plot showing standard free energy accompanying the transfer of one SDS molecule from a singly-dispersed state in the bulk aqueous phase to the assembled state ( $\Delta G_1^\circ$ ) as a function of the hydrocarbon tail length ( $n$ ) of the cationic surfactant molecules.

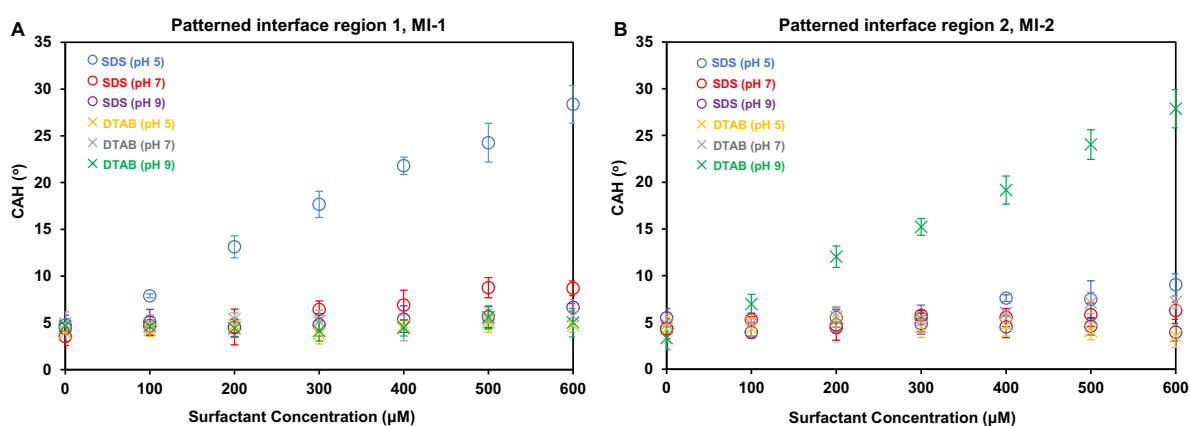


**Figure S12.** (A, B) The CAH of oil droplets on the (A) MI-1 portion and the (B) MI-2 portion of the patterned superoleophobic coating as a function of surfactant concentration at different pH values. Error bars represent standard deviations with  $n = 3$  for each data point. The volume of the beaded oil droplets was  $5 \mu\text{L}$ .

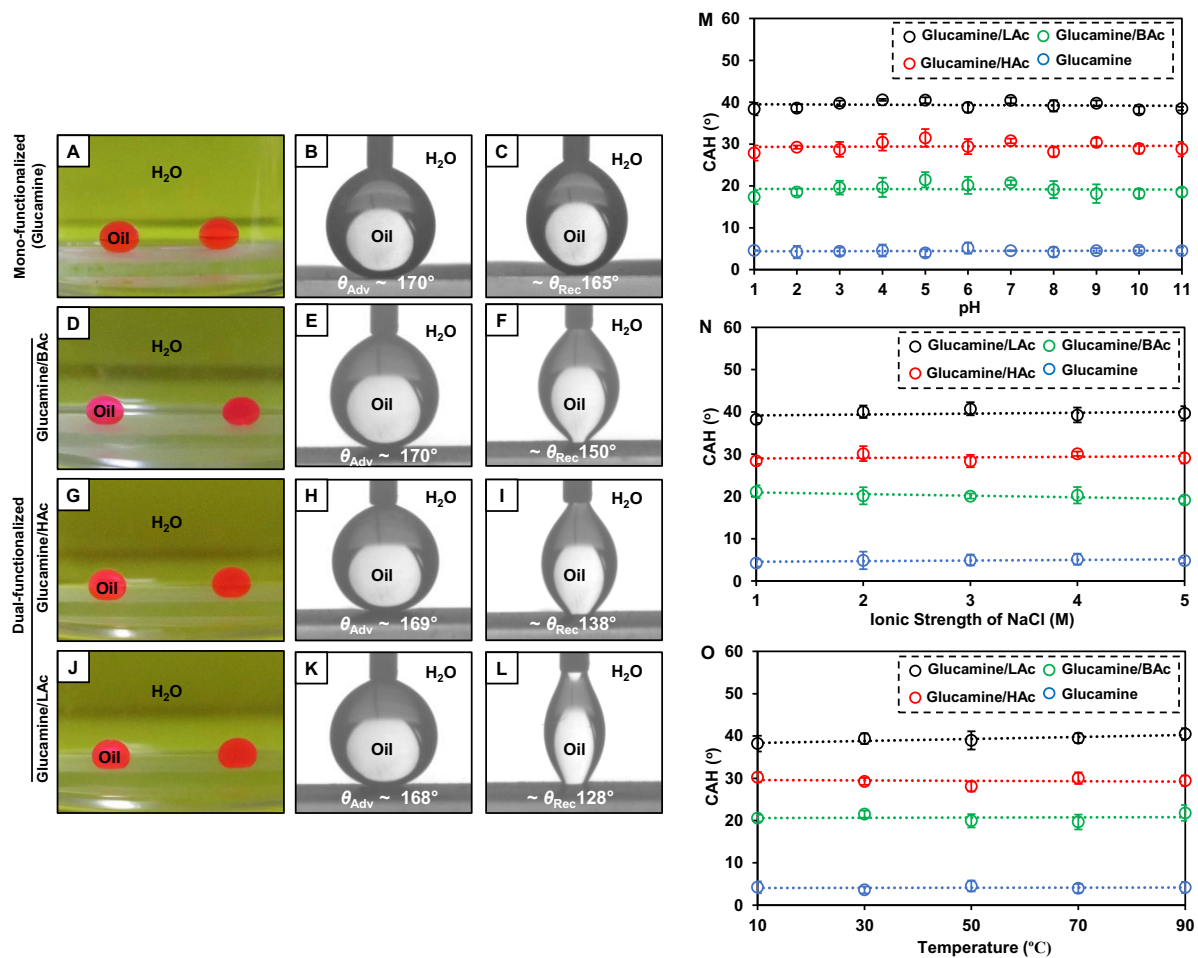


**Figure S13.** (A–L) Photographs (A, D, G, and J), and advancing (B, E, H, and K) and receding (C, F, I, and L) contact angle goniometer images of oil droplets (red-dye) on the mono-modified (Glucamine) and dual-modified (Glucamine/butyl acrylate (BAC), Glucamine/hexyl acrylate (HAc), and Glucamine/lauryl acrylate (LAc)) superoleophobic surfaces. (M–O) Figures detailing the independence of the CAH of the oil droplets with respect to the pH (M), NaCl concentration (N), and temperature (O). Error bars represent standard deviations with  $n = 3$  for each data point. The volumes of the beaded oil droplets were  $15 \mu\text{L}$  and  $5 \mu\text{L}$  for photographs and contact angle goniometer images, respectively.

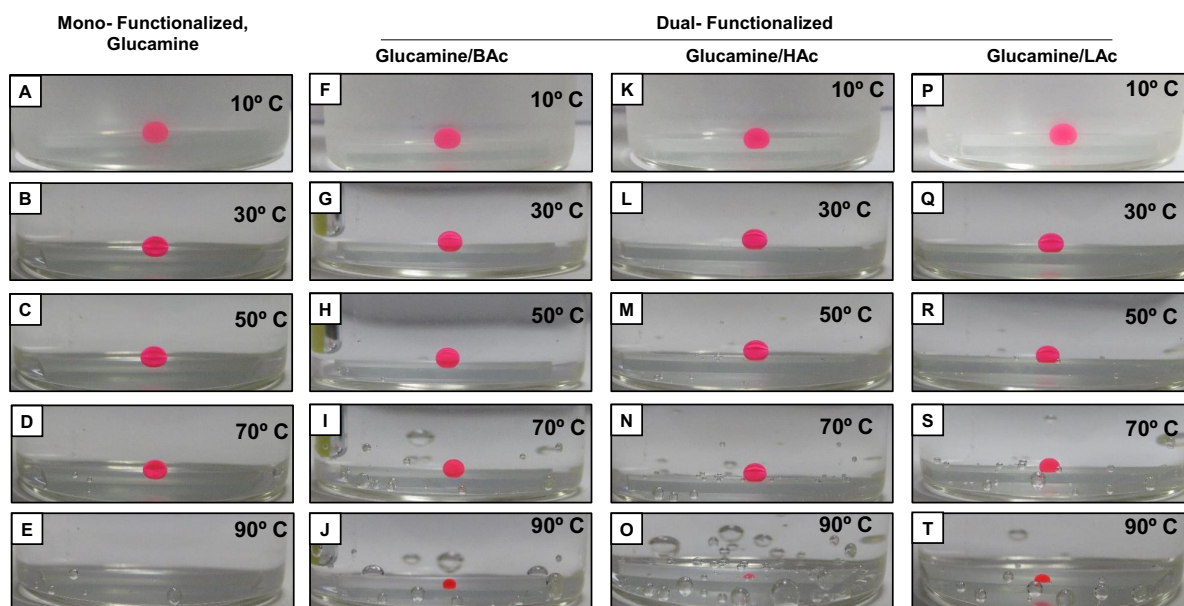


**Figure S14.** (A–T) Photographs of the effect of the temperature of the aqueous phase on the wetting behavior of oil droplets on the mono-functionalized (Glucamine, A–E) and dual-functionalized (Glucamine/butyl acrylate (BAC), F–J; Glucamine/hexyl acrylate (HAC), K–O; Glucamine/lauryl acrylate (LAC), P–T) superoleophobic coatings. The volume of the beaded oil droplets was 15  $\mu\text{L}$ .

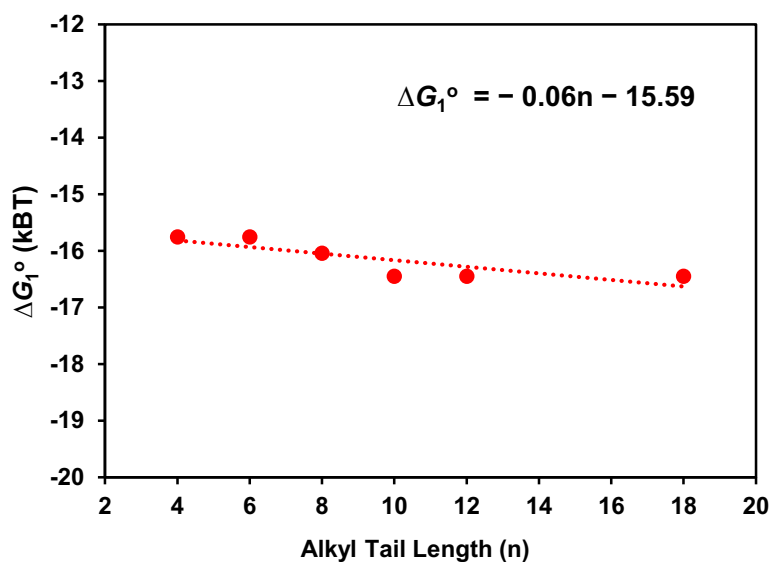


**Figure S15.** Plot showing standard free energy accompanying the transfer of one cholic acid molecule from a singly-dispersed state in the bulk aqueous phase to the assembled state ( $\Delta G_1^\circ$ ) as a function of the alkyltail length (n) of the glucamine/alkyl acrylate-modified coatings.

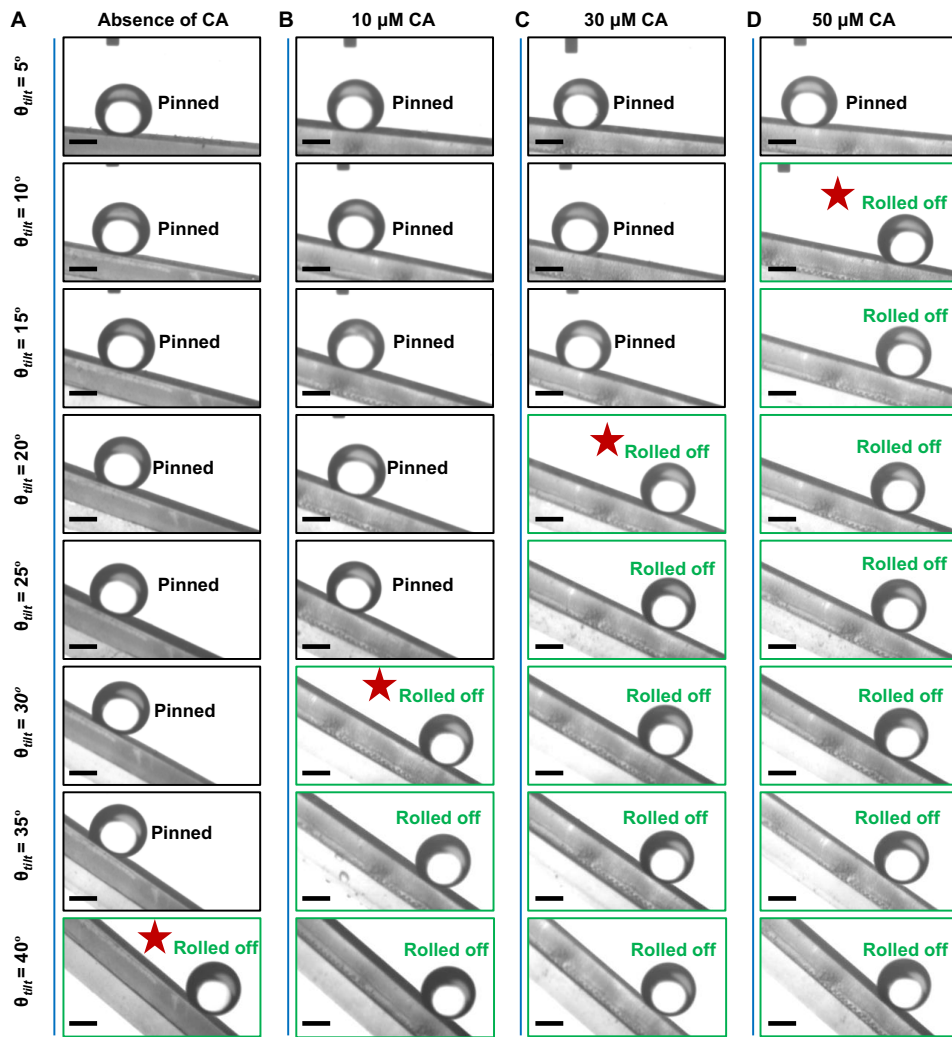


**Figure S16.** Photographs of the mobility of oil droplets on glucamine/lauryl acrylate–modified superoleophobic coatings as a function of cholic acid (CA) concentration. The red stars indicate the minimum tilting angle where the oil droplets started rolling off. The volume of the beaded oil droplets was 5  $\mu\text{L}$ . Scale bars, 1 mm.

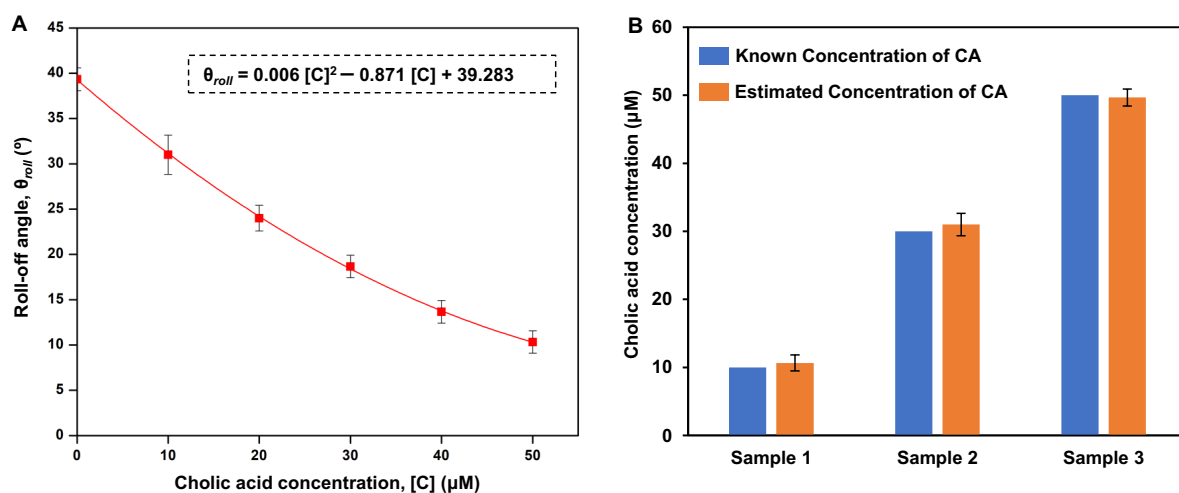


**Figure S17.** (A) Rolling-off angle ( $\theta_{roll}$ ) of oil droplets on glucamine/lauryl acrylate-modified superoleophobic coatings as a function of cholic acid concentration, [C]. The calibration curve is listed in the plot. (B) Estimation of the cholic acid concentration using the calibration curve in (A). Error bars represent standard deviations with  $n = 3$  for each data point. The volume of the beaded oil droplets was  $5 \mu\text{L}$ .

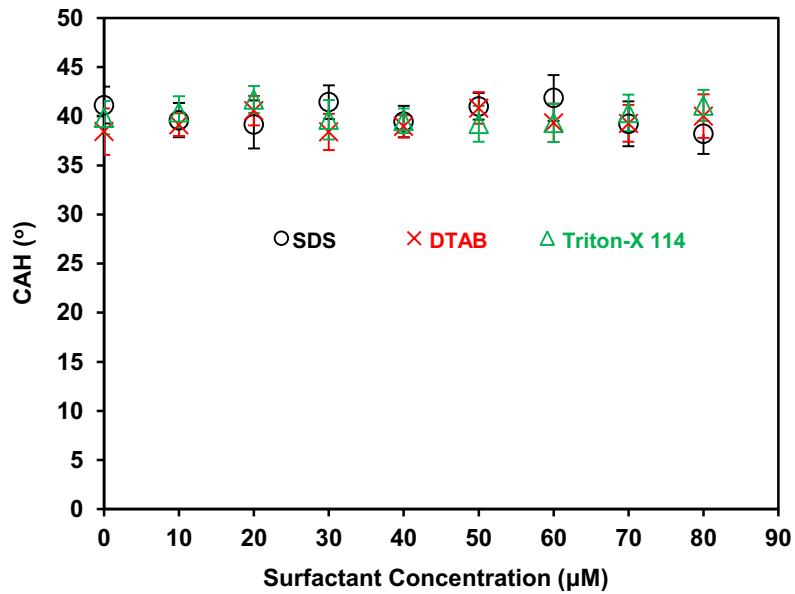


**Figure S18.** The CAH of oil droplets on the Glucamine/lauryl acrylate–modified superoleophobic coating as a function of anionic (SDS), cationic (DTAB), and non–ionic (Triton–X 114) surfactant concentration at aneutral pH. Error bars represent standard deviations with  $n = 3$  for each data point. The volume of the beaded oil droplets was  $5 \mu\text{L}$ .

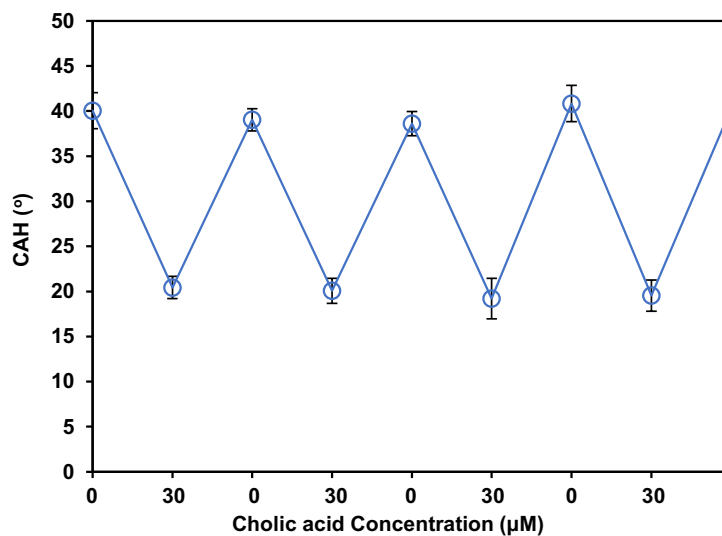


**Figure S19.** Reversible manipulation of the CAH on the glucamine/lauryl acrylate–modified superoleophobic coatings in aqueous solutions of cholic acid by switching its concentration between  $0$  and  $30 \mu\text{M}$ . Error bars represent standard deviations with  $n = 3$  for each data point. The volume of the beaded oil droplets was  $5 \mu\text{L}$ .